Automatica 44 (2008) 2517–2527

Contents lists available at ScienceDirect

Automatica

journal homepage: www.elsevier.com/locate/automatica

Magnetohydrodynamic state estimation with boundary sensors☆

Rafael Vazquez [a], Eugenio Schuster [b], Miroslav Krstic [c,*]

[a] Departamento de Ingeniería Aeroespacial, Universidad de Sevilla, 41092 Seville, Spain

[b] Department of Mechanical Engineering and Mechanics, Lehigh University, Bethlehem, PA 18015-1835, United States

[c] Department of Mechanical and Aerospace Engineering, University of California San Diego, La Jolla, CA 92093-0411, United States

ARTICLE INFO

Article history:
Received 10 September 2006
Received in revised form
20 August 2007
Accepted 25 February 2008
Available online 11 September 2008

Keywords:
Distributed parameter systems
Flow control
Nonlinear estimation
Spatial invariance
Partial differential equations

ABSTRACT

We present a PDE observer that estimates the velocity, pressure, electric potential and current fields in a magnetohydrodynamic (MHD) channel flow, also known as Hartmann flow. This flow is characterized by an electrically conducting fluid moving between parallel plates in the presence of an externally imposed transverse magnetic field. The system is described by the inductionless MHD equations, a combination of the Navier–Stokes equations and a Poisson equation for the electric potential under the so-called inductionless MHD approximation in a low magnetic Reynolds number regime. We identify physical quantities (measurable on the wall of the channel) that are sufficient to generate convergent estimates of the velocity, pressure, and electric potential field away from the walls. Our observer consists of a copy of the linearized MHD equations, combined with linear injection of output estimation error, with observer gains designed using backstepping. Pressure, skin friction and current measurements from one of the walls are used for output injection. For zero magnetic field or nonconducting fluid, the design reduces to an observer for the Navier–Stokes Poiseuille flow, a benchmark for flow control and turbulence estimation. We show that for the linearized MHD model the estimation error converges to zero in the L^2 norm. Despite being a subject of practical interest, the problem of observer design for nondiscretized 3-D MHD or Navier–Stokes channel flow has so far been an open problem.

1. Introduction

Recent years have been marked by dramatic advances in active flow control, but developments have had little effect on conducting fluids moving in magnetic fields. There are some recent results in stabilization though, for instance using nonlinear model reduction (Baker & Christofides, 2002), open-loop control (Berger, Kim, Lee, & Lim, 2000) and optimal control (Debbagh, Cathalifaud, & Airiau, 2007). Some experimental results are available, showing that control of such flows is technologically feasible; actuators consist of magnets and electrodes (Breuer & Park, 2004; Pang & Choi, 2004; Thibault & Rossi, 2003). Mathematical studies of controllability of magnetohydrodynamic flows have been done, though they do not provide explicit controllers (Barbu, Popa, Havarneanu, & Sritharan, 2003; Sritharan, Barbu, Havarneanu, & Popa, 2005). Despite being a subject of obvious practical interest, there are no previous results focusing on estimation of the velocity and electromagnetic fields for conducting fluids.

In this paper, we consider an incompressible MHD channel flow, also known as the Hartmann flow, a benchmark model for applications such as cooling systems (computer systems, fusion reactors), hypersonic flight, propulsion and laser applications. In this flow, an electrically conducting fluid moves between parallel plates and is affected by an imposed transverse magnetic field. When a conducting fluid moves in the presence of a magnetic field, it produces an electric field due to charge separation and subsequently an electric current. The interaction between this created electric current and the imposed magnetic field originates a body force, called the Lorentz force, which acts on the fluid itself. The velocity and electromagnetic fields are mathematically described by the MHD equations (Muller & Buhler, 2001; Sermange & Temam, 1983), which are the Navier–Stokes equations coupled with the Maxwell equations.

Our observer obtains an estimate of the whole velocity, pressure, electric potential and current fields, derived only from wall measurements. Obtaining such an estimate can be of interest in itself, depending on the application. For example, the absence of effective state estimators modeling turbulent fluid flows is considered one of the key obstacles to reliable, model-based weather forecasting. In other engineering applications in which

☆ This work was supported by NSF grant number CMS-0329662. This paper was not presented at any IFAC meeting. This paper was recommended for publication in revised form by Associate Editor Andrew R. Teel under the direction of Editor Hassan K. Khalil.

* Corresponding author. Tel.: +1 858 822 1374; fax: +1 858 822 3107.
E-mail addresses: rvazquez1@us.es (R. Vazquez), schuster@lehigh.edu (E. Schuster), krstic@ucsd.edu (M. Krstic).

0005-1098/$ – see front matter © 2008 Elsevier Ltd. All rights reserved.
doi:10.1016/j.automatica.2008.02.022

active control is needed, such as drag reduction (Pang & Choi, 2004) or mixing enhancement for cooling systems (Schuster & Krstic, 2003), designs usually assume unrealistic full state knowledge, therefore a state estimator is necessary for effective implementation.

This paper extends our previous work for estimation of the velocity field in a 2-D channel flow (Vazquez & Krstic, 2005). Our observer is designed for the continuum MHD model and consists of a copy of the plant together with output injection of measurement error. We identify which physical quantities (measurable on the wall of the channel) are sufficient to generate convergent estimates of the velocity, pressure, and electric potential field away from the walls. The main idea of the design is to apply the observer backstepping design method for parabolic PDEs (Smyshlyaev & Krstic, 2005) to the estimator error system; this system is similar to the Orr–Sommerfeld–Squire system of PDE's and presents the same difficulties (nonnormality leading to a large transient growth mechanism (Jovanovic & Bamieh, 2005; Schmid & Henningson, 2001)). Thus, applying the same ideas as in Cochran, Vazquez, and Krstic (2006), we use Fourier transform methods and some of the output injection gains to cast the system in a form where backstepping is applicable. Then, we design the remaining output injection gains not only to guarantee stability but also to decouple the system in order to prevent transients. The output injection gains can be computed solving linear hyperbolic PDEs—a much simpler task than, for instance, solving nonlinear Riccati equations (Smyshlyaev & Krstic, 2004). The observer needs measurements of pressure, skin friction and current at only one of the channel walls.

If the fluid is not conductive, or there is no magnetic field, the problem reduces to the Poiseuille channel flow problem and our observer design still holds. Frequently cited as a paradigm for transition to turbulence (Schmid & Henningson, 2001), the Poiseuille flow is a prototypical problem for flow control and turbulence estimation. There are many results in channel flow stabilization, for instance, using optimal control (Hogberg, Bewley, & Henningson, 2003), backstepping (Vazquez & Krstic, 2007), spectral decomposition/pole placement (Barbu, 2006; Triggiani, 2007), Lyapunov design/passivity (Aamo & Krstic, 2002; Balogh, Liu, & Krstic, 2001), or nonlinear model reduction/in-domain actuation (Baker, Armaou, & Christofides, 2000). Observer designs are more scarce; apart from the continuum backstepping approach (Vazquez & Krstic, 2005), previous works were in the form of an Extended Kalman Filter for the spatially discretized Navier–Stokes equations, employing high-dimensional algebraic Riccati equations for computation of observer gains (Chevalier, Hoepffner, Bewley, & Henningson, 2006; Hoepffner, Chevalier, Bewley, & Henningson, 2005).

The paper is organized as follows. Section 2 introduces the governing equations of our system. The equilibrium profile is presented in Section 3 and the observer structure and measurements are introduced in Section 4. Section 5 presents the design of the output injection gains to guarantee convergence of the observer estimates. In Section 6 we present a nonlinear estimator based on the linear design. We finish the paper with some concluding remarks in Section 7.

2. Model of the Hartmann flow

Consider an incompressible conducting fluid enclosed between two plates, separated by a distance L, under the influence of a pressure gradient ∇P and a magnetic field B_0 normal to the walls, as shown in Fig. 1. Under the assumption of a very small magnetic Reynolds number

$$Re_M = \nu\rho\sigma U_0 L \ll 1, \tag{1}$$

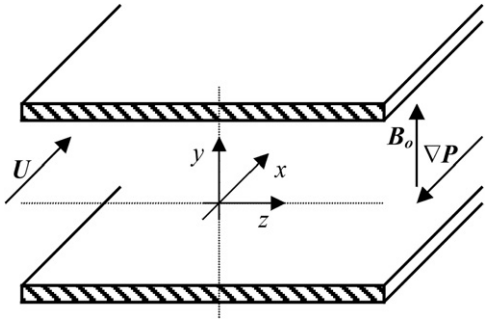

Fig. 1. Hartmann flow.

where ν is the viscosity of the fluid, ρ the density of the fluid, σ the conductivity of the fluid, and U_0 the reference velocity (maximum velocity of the equilibrium profile), the dynamics of the magnetic field can be neglected and the dimensionless velocity and electric potential field is governed by the inductionless MHD equations (Lee & Choi, 2001).

We set nondimensional coordinates (x, y, z), where x is the streamwise direction (parallel to the pressure gradient), y the wall normal direction (parallel to the magnetic field), z the spanwise direction, and where $(x, y, z) \in (-\infty, \infty)\times[0, 1]\times(-\infty, \infty)$. Let f_t denote the time derivative of a function f, similarly f_x, f_y and f_z the derivatives with respect to x, y and z, and define the 3-D Laplacian operator as $\triangle = \partial_{xx} + \partial_{yy} + \partial_{zz}$. The governing equations of the Hartmann flow are

$$U_t = \frac{\triangle U}{Re} - UU_x - VU_y - WU_z - P_x + N\phi_z - NU, \tag{2}$$

$$V_t = \frac{\triangle V}{Re} - UV_x - VV_y - WV_z - P_y, \tag{3}$$

$$W_t = \frac{\triangle W}{Re} - UW_x - VW_y - WW_z - P_z - N\phi_x - NW, \tag{4}$$

$$\triangle\phi = U_z - W_x, \tag{5}$$

where $U(t, x, y, z)$, $V(t, x, y, z)$ and $W(t, x, y, z)$ denote, respectively, the streamwise, wall-normal and spanwise velocities, $P(t, x, y, z)$ the pressure, $\phi(t, x, y, z)$ the electric potential, $Re = \frac{U_0 L}{\nu}$ is the Reynolds number and $N = \frac{\sigma L B_0^2}{\rho U_0}$ the Stuart number. Since the fluid is incompressible, the continuity equation is verified

$$U_x + V_y + W_z = 0. \tag{6}$$

The boundary conditions for the velocity field are

$$U(t, x, 0, z) = U(t, x, 1, z) = 0, \tag{7}$$

$$V(t, x, 0, z) = V(t, x, 1, z) = 0, \tag{8}$$

$$W(t, x, 0, z) = W(t, x, 1, z) = 0, \tag{9}$$

and assuming perfectly conducting walls, the electric potential must verify

$$\phi(t, x, 0, z) = \phi(t, x, 1, z) = 0. \tag{10}$$

The nondimensional electric current, $j(t, x, y, z)$, is a vector field that can be directly computed from the electric potential and velocity fields as follows,

$$j^x(t, x, y, z) = -\phi_x - W, \tag{11}$$

$$j^y(t, x, y, z) = -\phi_y, \tag{12}$$

$$j^z(t, x, y, z) = -\phi_z + U, \tag{13}$$

where j^x, j^y, and j^z denote the components of j.

Remark 1. If we set $N = 0$ (zero magnetic field, or nonconducting fluid) in Eqs. (2)–(5), they reduce to the classical Navier–Stokes equations without body forces. Then Eqs. (2)–(4) and (6)–(9) describe a pressure driven channel flow, the so-called Poiseuille flow.

3. Equilibrium profile

The equilibrium profile for system (2)–(5) can be calculated assuming a steady solution with only one nonzero nondimensional velocity component, U^e, that depends only on the y coordinate. Substituting U^e in Eq. (2), one finds that it verifies the following equation,

$$0 = \frac{U^e_{yy}(y)}{Re} - P^e_x - NU^e(y), \tag{14}$$

whose solution is, setting P^e such that the maximum velocity (centerline velocity) is 1,

$$U^e(y) = \frac{\sinh(H(1-y)) - \sinh H + \sinh(Hy)}{2\sinh H/2 - \sinh H}, \tag{15}$$

$$V^e = W^e = \phi^e = 0, \tag{16}$$

$$P^e = \frac{N\sinh H}{2\sinh H/2 - \sinh H}x, \tag{17}$$

$$j^{xe} = j^{ye} = 0, \tag{18}$$

$$j^{ze} = U^e(y), \tag{19}$$

where $H = \sqrt{Re\,N} = B_0 L\sqrt{\frac{\sigma}{\rho\nu}}$ is the Hartmann number. In Fig. 2 (left) we show $U^e(y)$ for different values of H. Note that the equilibrium profile is nondimensional so that the centerline velocity is always 1. For $H = 0$ the classic parabolic Poiseuille profile is recovered. In Fig. 2 (right) we show the equilibrium velocity gradient, $U^e_y(y)$, proportional to shear stress, whose maximum is reached at the boundaries and grows with H.

4. Observer

Define the fluctuation variables

$$u(t,x,y,z) = U(t,x,y,z) - U^e(y), \tag{20}$$

where $U^e(y)$ is the equilibrium of the Hartmann flow, as defined in (15). Define also $p(t,x,y,z) = P(t,x,y,z) - P^e(y)$ where $P^e(y)$ is defined in (17). We do not need to define fluctuation variables for V, W or ϕ since $V^e = W^e = \phi^e = 0$.

The linearization of (2)–(4) around the Hartmann equilibrium profile, written in the fluctuation variables (u, V, W, p, ϕ), is

$$u_t = \frac{\triangle u}{Re} - U^e(y)u_x - u^e_y(y)V - p_x + N\phi_z - NU, \tag{21}$$

$$V_t = \frac{\triangle V}{Re} - U^e(y)V_x - p_y, \tag{22}$$

$$W_t = \frac{\triangle W}{Re} - U^e(y)W_x - p_z - N\phi_x - NW. \tag{23}$$

Note that we don't need to linearize the potential Eq. (5), which using u is now $\triangle\phi = u_z - W_x$, or the continuity Eq. (6), which is $u_x + V_y + W_z = 0$, as they are already linear.

We design the observer for the linearized equations. It consists of a copy of (21)–(23) and (5)–(10), to which we add output injection of the pressure p, the potential flux ϕ_y (proportional to current), and both the streamwise and spanwise velocity gradients, u_y and W_y, (proportional to friction) at the bottom wall. We will show that this set of measurements (all of which are obtained from physically measurable quantities) is sufficient to generate convergent estimates of the velocity, pressure, and electric potential field away from the walls.

Denoting the observer (estimated) variables by a hat, the equations for the estimated velocity field are

$$\hat{u}_t = \frac{\triangle\hat{u}}{Re} - U^e(y)\hat{u}_x - U^e_y(y)\hat{V} - \hat{p}_x + N\hat{\phi}_z - N\hat{u} - Q^U, \tag{24}$$

$$\hat{V}_t = \frac{\triangle\hat{V}}{Re} - U^e(y)\hat{V}_x - \hat{p}_y - Q^V, \tag{25}$$

$$\hat{W}_t = \frac{\triangle\hat{W}}{Re} - U^e(y)\hat{W}_x - \hat{p}_z - N\hat{\phi}_x - N\hat{W} - Q^W. \tag{26}$$

The additional Q terms in the observer equation are related to output injection and defined as follows.

$$\begin{pmatrix} Q^U \\ Q^V \\ Q^W \end{pmatrix} = \int_{-\infty}^{\infty}\int_{-\infty}^{\infty} \mathbf{L}(x-\xi, y, z-\zeta) \times \begin{pmatrix} p(t,\xi,0,\zeta) - \hat{p}(t,\xi,0,\zeta) \\ u_y(t,\xi,0,\zeta) - \hat{u}_y(t,\xi,0,\zeta) \\ W_y(t,\xi,0,\zeta) - \hat{W}_y(t,\xi,0,\zeta) \\ \phi_y(t,\xi,0,\zeta) - \hat{\phi}_y(t,\xi,0,\zeta) \end{pmatrix} \mathrm{d}\xi\,\mathrm{d}\zeta, \tag{27}$$

where $\mathbf{L}$ is an output injection kernel matrix, defined as

$$\mathbf{L} = \begin{pmatrix} L^{UP} & L^{UU} & L^{UW} & L^{U\phi} \\ L^{VP} & L^{VU} & L^{VW} & L^{V\phi} \\ L^{WP} & L^{WU} & L^{WW} & L^{W\phi} \end{pmatrix}, \tag{28}$$

whose entries (which are functions of space) will be determined to ensure observer convergence. The estimated potential is computed from

$$\triangle\hat{\phi} = \hat{u}_z - \hat{W}_x, \tag{29}$$

and the observer verifies the continuity equation,

$$\hat{u}_x + \hat{V}_y + \hat{W}_z = 0, \tag{30}$$

and Dirichlet boundary conditions,

$$\hat{u}(t,x,0,z) = \hat{W}(t,x,0,z) = \hat{V}(t,x,0,z) = 0, \tag{31}$$

$$\hat{u}(t,x,1,z) = \hat{W}(t,x,1,z) = \hat{V}(t,x,1,z) = 0, \tag{32}$$

$$\hat{\phi}(t,x,0,z) = \hat{\phi}(t,x,1,z) = 0. \tag{33}$$

The estimated current field is computed from the other estimated variables using a copy of Eqs. (11)–(13).

$$\hat{j}^x(t,x,y,z) = -\hat{\phi}_x - \hat{W}, \tag{34}$$

$$\hat{j}^y(t,x,y,z) = -\hat{\phi}_y, \tag{35}$$

$$\hat{j}^z(t,x,y,z) = -\hat{\phi}_z + \hat{u}. \tag{36}$$

Remark 2. Note that the observer Eqs. (24)–(36) can be regarded as forced MHD equations, with the output injection acting as a body force. This means that any standard scheme for solving the forced MHD equations can be used to implement the observer, once the gains $\mathbf{L}$ in (28) have been calculated, as explained in the next section (the gains can be pre-computed before running the observer, and do not need to be updated afterwards).

Remark 3. As inputs to the observer, appearing in (27), one needs measurements of pressure, skin friction and current in the lower wall. For obtaining these measurements, pressure, skin friction and current sensors have to be embedded into one of the walls. Pressure and skin friction sensors are common in flow control, while for current measurement one could use an array of discrete current sensors, as depicted in Fig. 3.

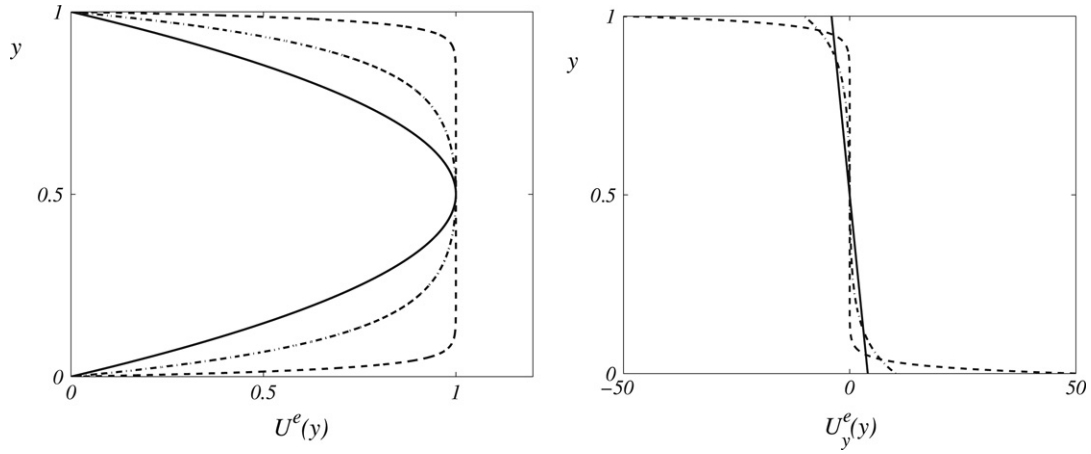

Fig. 2. Streamwise equilibrium velocity (left) and gradient of streamwise equilibrium velocity (right), for different values of H. Solid, $H = 0$; dash-dotted, $H = 10$; dashed, $H = 50$.

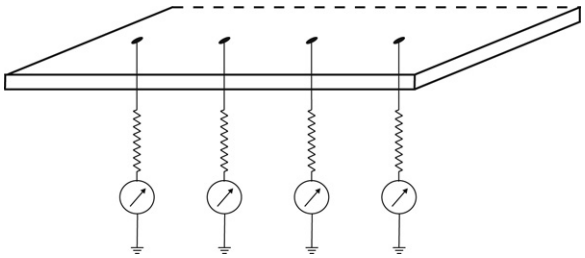

Fig. 3. An array of current sensors in the lower wall.

5. Observer design and convergence analysis

Subtracting the observer equations from the linearized plant equations we obtain the error equations, with states $\tilde{U} = u - \hat{u} = U - \hat{U}, \tilde{V} = V - \hat{V}, \tilde{W} = W - \hat{W}, \tilde{P} = p - \hat{p}, \tilde{\phi} = \phi - \hat{\phi}$,

$$\tilde{U}_t = \frac{\triangle \tilde{U}}{Re} - U^e(y)\tilde{U}_x - U^e_y(y)\tilde{V} - \tilde{P}_x + N\tilde{\phi}_z - N\tilde{U} + Q^U, \tag{37}$$

$$\tilde{V}_t = \frac{\triangle \tilde{V}}{Re} - U^e(y)\tilde{V}_x - \tilde{P}_y + Q^V, \tag{38}$$

$$\tilde{W}_t = \frac{\triangle \tilde{W}}{Re} - U^e(y)\tilde{W}_x - \tilde{P}_z - N\tilde{\phi}_x - N\tilde{W} + Q^W. \tag{39}$$

The observer error verifies the continuity equation,

$$\tilde{U}_x + \tilde{V}_y + \tilde{W}_z = 0, \tag{40}$$

while the potential error is governed by

$$\triangle\tilde{\phi} = \tilde{U}_z - \tilde{W}_x. \tag{41}$$

The boundary conditions for the error states are

$$\tilde{U}(t, x, 0, z) = \tilde{V}(t, x, 0, z) = \tilde{W}(t, x, 0, z) = 0, \tag{42}$$

$$\tilde{U}(t, x, 1, z) = \tilde{V}(t, x, 1, z) = \tilde{W}(t, x, 1, z) = 0, \tag{43}$$

$$\tilde{\phi}(t, x, 0, z) = \tilde{\phi}(t, x, 1, z) = 0. \tag{44}$$

To guarantee observer convergence, our design task is to design the output injection gains $\mathbf{L}$ defined in (27) that appear in Q^U, Q^V and Q^W, so that the origin of the error system is exponentially stable.

Since the observer error plant is linear and spatially invariant (Bamieh, Paganini, & Dahleh, 2000), we use a Fourier transform in the x and z coordinates (the spatially invariant directions). The transform pair (direct and inverse transform) is defined as

$$f(t, k_x, y, k_z) = \int_{-\infty}^{\infty}\int_{-\infty}^{\infty} f(t, x, y, z)\mathrm{e}^{-2\pi\mathrm{i}(k_x x + k_z z)}\mathrm{d}z\mathrm{d}x, \tag{45}$$

$$f(t, x, y, z) = \int_{-\infty}^{\infty}\int_{-\infty}^{\infty} f(t, k_x, y, k_z)\mathrm{e}^{2\pi\mathrm{i}(k_x x + k_z z)}\mathrm{d}k_z\mathrm{d}k_x. \tag{46}$$

Note that we use the same symbol f for both the original $f(t, x, y, z)$ and the image $f(t, k_x, y, k_z)$. In hydrodynamics k_x and k_z are referred to as the "wave numbers".

The observer error equations in Fourier space are

$$\begin{aligned}\tilde{U}_t = {} & \frac{-\alpha^2\tilde{U} + \tilde{U}_{yy}}{Re} - \beta\tilde{U} - U^e_y\tilde{V} - 2\pi k_x\mathrm{i}\tilde{P} + L^{UP}P_0 + L^{UU}U_{y0} \\ & + L^{UW}W_{y0} + L^{U\phi}\phi_{y0} + 2\pi k_z\mathrm{i}N\tilde{\phi} - N\tilde{U},\end{aligned} \tag{47}$$

$$\begin{aligned}\tilde{V}_t = {} & \frac{-\alpha^2\tilde{V} + \tilde{V}_{yy}}{Re} - \beta\tilde{V} - \tilde{P}_y \\ & + L^{VP}P_0 + L^{VU}U_{y0} + L^{VW}W_{y0} + L^{V\phi}\phi_{y0},\end{aligned} \tag{48}$$

$$\begin{aligned}\tilde{W}_t = {} & \frac{-\alpha^2\tilde{W} + W_{yy}}{Re} - \beta\tilde{W} - 2\pi k_z\mathrm{i}\tilde{P} + L^{WP}P_0 + L^{WU}U_{y0} \\ & + L^{WW}W_{y0} + L^{W\phi}\phi_{y0} - 2\pi k_x\mathrm{i}N\tilde{\phi} - N\tilde{W}\end{aligned} \tag{49}$$

where $\alpha^2 = 4\pi^2(k_x^2 + k_z^2)$, the L's are the entries of $\mathbf{L}$ in Fourier space, and where we have used the definition (27) of the output injection terms as convolutions, which become products in Fourier space. We have written for short $P_0 = \tilde{P}(t, k_x, 0, k_z)$, $U_{y0} = \tilde{U}_y(t, k_x, 0, k_z)$, $W_{y0} = \tilde{W}_y(t, k_x, 0, k_z)$, $\phi_{y0} = \tilde{\phi}_y(t, k_x, 0, k_z)$.

The continuity equation in Fourier space is expressed as

$$2\pi\mathrm{i}k_x\tilde{U} + \tilde{V}_y + 2\pi k_z\tilde{W} = 0, \tag{50}$$

and the equation for the potential is

$$-\alpha^2\tilde{\phi} + \hat{\phi}_{yy} = 2\pi\mathrm{i}\left(k_z\tilde{U} - k_x\tilde{W}\right). \tag{51}$$

Note that (47)–(51) is uncoupled for each wave number. This is due to spatial invariance (Bamieh et al., 2000) of the plant and linearity of the equations in physical space, (37)–(39). Hence, the observer gains can be determined *separately* for each pair of wave numbers k_x and k_z. For small wave numbers, verifying that $k_x^2 + k_z^2 \leq M^2$ for a parameter M that will be determined, we will design the output injection gains $\mathbf{L}$ to guarantee exponential stability of the origin of the error system (47)–(51), thus ensuring convergence of the estimates. We will refer to the wave number range $k_x^2 + k_z^2 \leq M^2$ as

the *observed* wave number range. For the rest of the wave numbers, that verify $k_x^2 + k_z^2 > M^2$, we will show that the origin of the error system (47)–(51) is already exponentially stable without output injection, so we just set $\mathbf{L} = \mathbf{0}$. We will refer to this wave number range as the *unobserved* wave number range. Once stability for all wave numbers (in both the observed and unobserved range) is established, stability in physical space follows (see Vazquez and Krstic (2007)). The number M is computed in Section 5.2 to ensure stability for the unobserved wave number range.

We define χ, a *truncating* function, as

$$\chi(k_x, k_z) = \begin{cases} 1, & k_x^2 + k_z^2 \leq M^2, \\ 0, & \text{otherwise.} \end{cases} \tag{52}$$

Then, we reflect that we don't use output injection for unobserved wave numbers by writing

$$\mathbf{L} = \chi(k_x, y, k_z)\mathbf{R}(k_x, y, k_x). \tag{53}$$

This can be written in physical space, using the definition of the Fourier transform, as

$$\mathbf{L}(x, y, z) = \int_{-\infty}^{\infty}\int_{-\infty}^{\infty} \chi(k_x, y, k_z)\mathbf{R}(k_x, y, k_z) \times \mathrm{e}^{2\pi \mathrm{i}(k_x x + k_z z)}\mathrm{d}k_z \mathrm{d}k_x. \tag{54}$$

The matrix $\mathbf{R}$ is defined as

$$\mathbf{R} = \begin{pmatrix} R^{UP} & R^{UU} & R^{UW} & R^{U\phi} \\ R^{VP} & R^{VU} & R^{VW} & R^{V\phi} \\ R^{WP} & R^{WU} & R^{WW} & R^{W\phi} \end{pmatrix}, \tag{55}$$

and using $\mathbf{R}$ we can write the observer error equations as

$$\begin{aligned} \tilde{U}_t &= \frac{-\alpha^2\tilde{U} + \tilde{U}_{yy}}{Re} - \beta\tilde{U} - U_y^e\tilde{V} - 2\pi k_x \mathrm{i}\tilde{P} + \chi(k_x, k_z) \\ &\quad \times \left\{R^{UP}P_0 + R^{UU}U_{y0} + R^{UW}W_{y0} + R^{U\phi}\phi_{y0}\right\} \\ &\quad + 2\pi k_z \mathrm{i}N\tilde{\phi} - N\tilde{U}, \end{aligned} \tag{56}$$

$$\begin{aligned} \tilde{V}_t &= \frac{-\alpha^2\tilde{V} + \tilde{V}_{yy}}{Re} - \beta\tilde{V} - \tilde{P}_y + \chi(k_x, k_z) \\ &\quad \times \left\{R^{VP}P_0 + R^{VU}U_{y0} + R^{VW}W_{y0}R^{V\phi}\phi_{y0}\right\}, \end{aligned} \tag{57}$$

$$\begin{aligned} \tilde{W}_t &= \frac{-\alpha^2\tilde{W} + W_{yy}}{Re} - \beta\tilde{W} - 2\pi k_z \mathrm{i}\tilde{P} + \chi(k_x, k_z) \\ &\quad \times \left\{R^{WP}P_0 + R^{WU}U_{y0} + R^{WW}W_{y0} + R^{W\phi}\phi_{y0}\right\} \\ &\quad - 2\pi k_x \mathrm{i}N\tilde{\phi} - N\tilde{W}. \end{aligned} \tag{58}$$

Note that once $\mathbf{R}$ is determined, we obtain $\mathbf{L}$ using (54).

5.1. Observed wave number analysis

Consider $k_x^2 + k_z^2 \leq M^2$. Then $\chi = 1$, so output injection is present. Using the continuity equation (50) and Eqs. (56)–(58), the following Poisson equation for the pressure is derived,

$$-\alpha^2\tilde{P} + \tilde{P}_{yy} = \Upsilon - 4\pi k_x \mathrm{i}U_y^e(y)\tilde{V} + NV_y, \tag{59}$$

where Υ contains all the terms due to output injection,

$$\begin{aligned} \Upsilon &= P_0\left(2\pi \mathrm{i}k_x R^{UP} + R_y^{VP} + 2\pi k_z R^{WP}\right) \\ &\quad + U_{y0}\left(2\pi \mathrm{i}k_x R^{UU} + R_y^{VU} + 2\pi k_z R^{WU}\right) \\ &\quad + W_{y0}\left(2\pi \mathrm{i}k_x R^{UW} + R_y^{VW} + 2\pi k_z R^{WW}\right) \\ &\quad + \phi_{y0}\left(2\pi \mathrm{i}k_x R^{U\phi} + R_y^{V\phi} + 2\pi k_z R^{W\phi}\right). \end{aligned} \tag{60}$$

We want to make (59) independent of the output injection gains, for which we need $\Upsilon = 0$. Hence, we set

$$\begin{aligned} R^{VP}(k_x, y, k_z) &= R^{VP}(k_x, 0, k_z) \\ &\quad - 2\pi \mathrm{i}\int_0^y \left(k_x R^{UP} + k_z R^{WP}\right)(k_x, \eta, k_z)\mathrm{d}\eta, \end{aligned} \tag{61}$$

$$\begin{aligned} R^{VU}(k_x, y, k_z) &= R^{VU}(k_x, 0, k_z) \\ &\quad - 2\pi \mathrm{i}\int_0^y \left(k_x R^{UU} + k_z R^{WU}\right)(k_x, \eta, k_z)\mathrm{d}\eta, \end{aligned} \tag{62}$$

$$\begin{aligned} R^{VW}(k_x, y, k_z) &= R^{VW}(k_x, 0, k_z) \\ &\quad - 2\pi \mathrm{i}\int_0^y \left(k_x R^{UW} + k_z R^{WW}\right)(k_x, \eta, k_z)\mathrm{d}\eta, \end{aligned} \tag{63}$$

$$\begin{aligned} R^{V\phi}(k_x, y, k_z) &= R^{V\phi}(k_x, 0, k_z) \\ &\quad - 2\pi \mathrm{i}\int_0^y \left(k_x R^{U\phi} + k_z R^{W\phi}\right)(k_x, \eta, k_z)\mathrm{d}\eta, \end{aligned} \tag{64}$$

which means that, in physical space, $\nabla \cdot \mathbf{L} = 0$. Hence, as Eq. (59) is derived by taking divergence of (56)–(58), the output injection terms cancel away.

Expression (59) can be solved in terms of the values of the pressure at the bottom wall.

$$\begin{aligned} \tilde{P} &= -\frac{4\pi k_x \mathrm{i}}{\alpha}\int_0^y U_y^e(\eta)\sinh(\alpha(y-\eta))\,\tilde{V}(t, k_x, \eta, k_z)\mathrm{d}\eta \\ &\quad + \cosh(\alpha y)\,P_0 + \frac{\sinh(\alpha y)}{\alpha}\tilde{P}_y(t, k_x, 0, k_z) \\ &\quad + N\int_0^y \frac{\sinh(\alpha(y-\eta))}{\alpha}\tilde{V}_y(t, k_x, \eta, k_z)\mathrm{d}\eta. \end{aligned} \tag{65}$$

Evaluating Eq. (57) at $y = 0$ one finds that

$$\begin{aligned} \tilde{P}_y(t, k_x, 0, k_z) &= \Upsilon_0 + \frac{\tilde{V}_{yy}(t, k_x, 0, k_z)}{Re} \\ &= \Upsilon_0 - 2\pi \mathrm{i}\frac{k_x U_{y0} + k_z \tilde{W}_{y0}}{Re}, \end{aligned} \tag{66}$$

where we have used (50) for expressing $\tilde{V}_{yy}$ at the bottom in terms of measurements. In (66),

$$\begin{aligned} \Upsilon_0 &= P_0 R^{VP}(k_x, 0, k_z) + U_{y0}R^{VU}(k_x, 0, k_z) \\ &\quad + W_{y0}R^{VW}(k_x, 0, k_z) + \phi_{y0}R^{V\phi}(k_x, 0, k_z), \end{aligned} \tag{67}$$

and as before we need the pressure to be independent of any output injection gains. Hence, we set

$$\begin{aligned} R^{VP}(k_x, 0, k_z) &= R^{VU}(k_x, 0, k_z) = R^{VW}(k_x, 0, k_z) \\ &= R^{V\phi}(k_x, 0, k_z) = 0. \end{aligned} \tag{68}$$

Then, the pressure can be expressed independently of the output injection gains in terms of a strict-feedback (Krstic, Kanellakopoulos, & Kokotovic, 1995) integral of the state $\tilde{V}$ and measurements,

$$\begin{aligned} \tilde{P} &= -\frac{4\pi k_x \mathrm{i}}{\alpha}\int_0^y U_y^e(\eta)\sinh(\alpha(y-\eta))\,\tilde{V}(t, k_x, \eta, k_z)\mathrm{d}\eta \\ &\quad + \cosh(\alpha y)\,P_0 - 2\pi \mathrm{i}\frac{\sinh(\alpha y)}{Re\alpha}\left(k_x U_{y0} + k_z W_{y0}\right) \\ &\quad + N\int_0^y \frac{\sinh(\alpha(y-\eta))}{\alpha}\tilde{V}_y(t, k_x, \eta, k_z)\mathrm{d}\eta. \end{aligned} \tag{69}$$

Similarly, solving for ϕ in terms of the measurement ϕ_{y0} and the right hand side of its Poisson Eq. (51),

$$\begin{aligned} \tilde{\phi} &= \frac{2\pi \mathrm{i}}{\alpha}\int_0^y \sinh(\alpha(y-\eta))\left(k_z\tilde{U}(t, k_x, \eta, k_z)\right. \\ &\quad \left. - k_x\tilde{W}(t, k_x, \eta, k_z)\right)\mathrm{d}\eta + \frac{\sinh(\alpha y)}{\alpha}\phi_{y0}. \end{aligned} \tag{70}$$

Introducing the expressions (69) and (70) in (56) and (58), we get

$$\begin{aligned}\tilde{U}_t &= \frac{-\alpha^2\tilde{U}+\tilde{U}_{yy}}{Re}-\beta\tilde{U}-U_y^e(y)\tilde{V}-N\tilde{U}\\ &\quad+P_0\left(R^{UP}-2\pi k_x\mathrm{i}\cosh(\alpha y)\right)\\ &\quad+U_{y0}\left(R^{UU}-\frac{4\pi^2k_x^2}{\alpha Re}\sinh(\alpha y)\right)\\ &\quad+W_{y0}\left(R^{UW}-\frac{4\pi^2k_xk_z}{\alpha Re}\sinh(\alpha y)\right)\\ &\quad+\phi_{y0}\left(R^{U\phi}+N\frac{2\pi k_z\mathrm{i}}{\alpha}\sinh(\alpha y)\right)\\ &\quad-\frac{8\pi k_x^2}{\alpha}\int_0^y U_y^e(\eta)\sinh(\alpha(y-\eta))\,\tilde{V}(t,k_x,\eta,k_z)\mathrm{d}\eta\\ &\quad-2\pi\mathrm{i}k_xN\int_0^y\frac{\sinh(\alpha(y-\eta))}{\alpha}\tilde{V}_y(t,k_x,\eta,k_z)\mathrm{d}\eta\\ &\quad-\frac{4\pi^2k_zN}{\alpha}\int_0^y\sinh(\alpha(y-\eta))\\ &\quad\times\left(k_z\tilde{U}(t,k_x,\eta,k_z)-k_x\tilde{W}(t,k_x,\eta,k_z)\right)\mathrm{d}\eta, \end{aligned}\tag{71}$$

$$\begin{aligned}\tilde{W}_t &= \frac{-\alpha^2\tilde{W}+W_{yy}}{Re}-\beta\tilde{W}-N\tilde{W}\\ &\quad+P_0\left(R^{WP}-2\pi k_z\mathrm{i}\cosh(\alpha y)\right)\\ &\quad+U_{y0}\left(R^{WU}-\frac{4\pi^2k_xk_z}{\alpha Re}\sinh(\alpha y)\right)\\ &\quad+W_{y0}\left(R^{WW}-\frac{4\pi^2k_z^2}{\alpha Re}\sinh(\alpha y)\right)\\ &\quad+\phi_{y0}\left(R^{W\phi}-N\frac{2\pi k_xi}{\alpha}\sinh(\alpha y)\right)\\ &\quad-\frac{8\pi k_xk_z}{\alpha}\int_0^y U_y^e(\eta)\sinh(\alpha(y-\eta))\,\tilde{V}(t,k_x,\eta,k_z)\mathrm{d}\eta\\ &\quad-2\pi\mathrm{i}k_zN\int_0^y\frac{\sinh(\alpha(y-\eta))}{\alpha}\tilde{V}_y(t,k_x,\eta,k_z)\mathrm{d}\eta\\ &\quad+\frac{4\pi^2k_xN}{\alpha}\int_0^y\sinh(\alpha(y-\eta))\\ &\quad\times\left(k_z\tilde{U}(t,k_x,\eta,k_z)-k_x\tilde{W}(t,k_x,\eta,k_z)\right)\mathrm{d}\eta. \end{aligned}\tag{72}$$

Note that we have omitted the equation for $\tilde{V}$ since, from (50) and using the fact that $\tilde{V}(t,k_x,0,k_z)=0$, $\tilde{V}$ is computed from $\tilde{U}$ and $\tilde{W}$:

$$\tilde{V}=-2\pi\mathrm{i}\int_0^y\left(k_x\tilde{U}(t,k_x,\eta,k_z)+k_z\tilde{W}(t,k_x,\eta,k_z)\right)\mathrm{d}\eta.\tag{73}$$

We now set the output injection terms to directly cancel the boundary terms coming from (69) and (70), while still leaving some additional gains to stabilize the system. Thus, we define

$$R^{UP}=2\pi k_x\mathrm{i}\cosh(\alpha y),\tag{74}$$

$$R^{WP}=2\pi k_z\mathrm{i}\cosh(\alpha y),\tag{75}$$

$$R^{UU}=\frac{4\pi^2k_x^2}{\alpha Re}\sinh(\alpha y)+\Pi_1(k_x,y,k_z),\tag{76}$$

$$R^{WU}=\frac{4\pi^2k_xk_z}{\alpha Re}\sinh(\alpha y)+\Pi_2(k_x,y,k_z),\tag{77}$$

$$R^{UW}=\frac{4\pi^2k_xk_z}{\alpha Re}\sinh(\alpha y)+\Pi_3(k_x,y,k_z),\tag{78}$$

$$R^{WW}=\frac{4\pi^2k_z^2}{\alpha Re}\sinh(\alpha y)+\Pi_4(k_x,y,k_z),\tag{79}$$

$$R^{U\phi}=-N\frac{2\pi k_z\mathrm{i}}{\alpha}\sinh(\alpha y),\tag{80}$$

$$R^{W\phi}=N\frac{2\pi k_x\mathrm{i}}{\alpha}\sinh(\alpha y),\tag{81}$$

where the gains Π_1, Π_2, Π_3 and Π_4 are to be defined later. From (61)–(64), (68) and (74)–(81), we get a explicit expression for the remaining entries of $\mathbf{R}$,

$$R^{VP}=\alpha\sinh(\alpha y),\tag{82}$$

$$\begin{aligned}R^{VU} &= 2\pi\mathrm{i}(k_x+k_z)\frac{1-\cosh(\alpha y)}{Re}-2\pi\mathrm{i}\\ &\quad\times\int_0^y(k_x\Pi_1(k_x,\eta,k_z)+k_z\Pi_2(k_x,\eta,k_z))\,\mathrm{d}\eta,\end{aligned}\tag{83}$$

$$\begin{aligned}R^{VW} &= 2\pi\mathrm{i}(k_x+k_z)\frac{1-\cosh(\alpha y)}{Re}-2\pi\mathrm{i}\\ &\quad\times\int_0^y(k_x\Pi_3(k_x,\eta,k_z)+k_z\Pi_4(k_x,\eta,k_z))\,\mathrm{d}\eta,\end{aligned}\tag{84}$$

$$R^{V\phi}=0.\tag{85}$$

Introducing (74)–(85) in Eqs. (71) and (72) we get

$$\begin{aligned}\tilde{U}_t &= \frac{-\alpha^2\tilde{U}+\tilde{U}_{yy}}{Re}-\beta\tilde{U}-U_y^e(y)\tilde{V}-N\tilde{U}\\ &\quad+\Pi_1U_{y0}+\Pi_3W_{y0}-\frac{4\pi^2k_zN}{\alpha}\int_0^y\sinh(\alpha(y-\eta))\\ &\quad\times\left(k_z\tilde{U}(t,k_x,\eta,k_z)-k_x\tilde{W}(t,k_x,\eta,k_z)\right)\mathrm{d}\eta\\ &\quad-\frac{8\pi k_x^2}{\alpha}\int_0^y U_y^e(\eta)\sinh(\alpha(y-\eta))\,\tilde{V}(t,k_x,\eta,k_z)\mathrm{d}\eta\\ &\quad-2\pi\mathrm{i}k_xN\int_0^y\frac{\sinh(\alpha(y-\eta))}{\alpha}\tilde{V}_y(t,k_x,\eta,k_z)\mathrm{d}\eta,\end{aligned}\tag{86}$$

$$\begin{aligned}\tilde{W}_t &= \frac{-\alpha^2\tilde{W}+W_{yy}}{Re}-\beta\tilde{W}-N\tilde{W}+\Pi_2U_{y0}+\Pi_4W_{y0}\\ &\quad-\frac{8\pi k_xk_z}{\alpha}\int_0^y U_y^e(\eta)\sinh(\alpha(y-\eta))\,\tilde{V}(t,k_x,\eta,k_z)\mathrm{d}\eta\\ &\quad-2\pi\mathrm{i}k_zN\int_0^y\frac{\sinh(\alpha(y-\eta))}{\alpha}\tilde{V}_y(t,k_x,\eta,k_z)\mathrm{d}\eta\\ &\quad+\frac{4\pi^2k_xN}{\alpha}\int_0^y\sinh(\alpha(y-\eta))\\ &\quad\times\left(k_z\tilde{U}(t,k_x,\eta,k_z)-k_x\tilde{W}(t,k_x,\eta,k_z)\right)\mathrm{d}\eta.\end{aligned}\tag{87}$$

Now, we introduce the following change of variables and its inverse,

$$Y=2\pi\mathrm{i}\left(k_x\tilde{U}+k_z\tilde{W}\right),\qquad\omega=2\pi\mathrm{i}\left(k_z\tilde{U}-k_x\tilde{W}\right),\tag{88}$$

$$\tilde{U}=\frac{2\pi\mathrm{i}}{\alpha^2}(k_xY+k_z\omega),\qquad\tilde{W}=\frac{2\pi\mathrm{i}}{\alpha^2}(k_zY-k_x\omega).\tag{89}$$

Defining $\epsilon=\frac{1}{Re}$ and the following functions

$$\beta(k_x,y)=2\pi\mathrm{i}k_xU^e(y),\tag{90}$$

$$\begin{aligned}f(k_x,y,\eta,k_z) &= 4\pi\mathrm{i}k_x\left\{\frac{U_y^e(y)}{2}+\int_\eta^y\frac{\sinh(\alpha(y-\sigma))}{\alpha}\right.\\ &\quad\left.\times U_y^e(\sigma)\mathrm{d}\sigma\right\}+N\alpha\sinh(\alpha(y-\eta)),\end{aligned}\tag{91}$$

$$h_1(y,k_z)=2\pi\mathrm{i}k_zU_y^e(y),\tag{92}$$

$$h_2(k_x,y,\eta,k_z)=-N\alpha\sinh(\alpha(y-\eta)).\tag{93}$$

Eqs. (86) and (87) expressed in terms of Y and ω are

$$\begin{aligned} Y_t &= \epsilon\left(-\alpha^2 Y + Y_{yy}\right) - \beta Y - NY \\ &\quad + \frac{4\pi^2}{\alpha^2}\left(k_x^2\Pi_1 + k_x k_z \Pi_2 + k_x k_z \Pi_3 + k_z^2 \Pi_4\right) Y_{y0} \\ &\quad + \frac{4\pi^2}{\alpha^2}\left(k_x k_z \Pi_1 + k_z^2 \Pi_2 - k_x^2 \Pi_3 - k_x k_z \Pi_4\right) \omega_{y0} \\ &\quad + \int_0^y f(k_x, y, \eta, k_z) Y(t, k_x, \eta, k_z)\mathrm{d}\eta, \end{aligned} \tag{94}$$

$$\begin{aligned} \omega_t &= \epsilon\left(-\alpha^2 \omega + \omega_{yy}\right) - \beta\omega - N\omega \\ &\quad + \frac{4\pi^2}{\alpha^2}\left(k_x k_z \Pi_1 - k_x^2 \Pi_2 + k_z^2 \Pi_3 - k_x k_z \Pi_4\right) Y_{y0} \\ &\quad + \frac{4\pi^2}{\alpha^2}\left(k_z^2 \Pi_1 - k_x k_z \Pi_2 - k_x k_z \Pi_3 + k_x^2 \Pi_4\right) \omega_{y0} \\ &\quad + h_1(y, k_z) \int_0^y Y(t, k_x, \eta, k_z)\mathrm{d}\eta \\ &\quad + \int_0^y h_2(k_x, y, \eta, k_z)\omega(t, k_x, \eta, k_z)\mathrm{d}\eta, \end{aligned} \tag{95}$$

where we have used the inverse change of variables (89) to express U_{y0} and W_{y0} in terms of $Y_{y0} = Y(t, k_x, 0, k_z)$ and $\omega_{y0} = \omega(t, k_x, 0, k_z)$. We define now the output injection gains Π_1, Π_2, Π_3 and Π_4 in the following way

$$\begin{pmatrix} \Pi_1 \\ \Pi_2 \\ \Pi_3 \\ \Pi_4 \end{pmatrix} = \mathbf{A}^{-1} \begin{pmatrix} l(k_x, y, 0, k_z) \\ 0 \\ \theta_1(k_x, y, 0, k_z) \\ \theta_2(k_x, y, 0, k_z) \end{pmatrix}. \tag{96}$$

The matrix $\mathbf{A}$ is defined as

$$\mathbf{A} = \frac{4\pi^2}{\alpha^2} \begin{pmatrix} k_x^2 & k_x k_z & k_x k_z & k_z^2 \\ k_x k_z & k_z^2 & -k_x^2 & -k_x k_z \\ k_x k_z & -k_x^2 & k_z^2 & -k_x k_z \\ k_z^2 & -k_x k_z & -k_x k_z & k_x^2 \end{pmatrix}, \tag{97}$$

and since $\det(\mathbf{A}) = -1$ its inverse appearing in Eq. (96) is well-defined, whereas the functions $l(k_x, y, \eta, k_z)$, $\theta_1(k_x, y, \eta, k_z)$, and $\theta_2(k_x, y, \eta, k_z)$ in (96) are to be found. Using (96), Eqs. (94) and (95) become

$$\begin{aligned} Y_t &= \epsilon\left(-\alpha^2 Y + Y_{yy}\right) - \beta Y - NY + l(k_x, y, 0, k_z) Y_{y0} \\ &\quad + \int_0^y f(k_x, y, \eta, k_z) Y(k_x, \eta, k_z)\mathrm{d}\eta, \end{aligned} \tag{98}$$

$$\begin{aligned} \omega_t &= \epsilon\left(-\alpha^2 \omega + \omega_{yy}\right) - \beta\omega - N\omega + \theta_1(k_x, y, 0, k_z) Y_{y0} \\ &\quad + \theta_2(k_x, y, 0, k_z)\omega_{y0} + h_1 \int_0^y Y(k_x, \eta, k_z)\mathrm{d}\eta \\ &\quad + \int_0^y h_2(k_x, y, \eta, k_z)\omega(k_x, \eta, k_z)\mathrm{d}\eta. \end{aligned} \tag{99}$$

Eqs. (98) and (99) are a coupled, strict-feedback plant, with integral and reaction terms. A variant of the design presented in Smyshlyaev and Krstic (2005) can be used to design the gains $l(k_x, y, 0, k_z)$, $\theta_1(k_x, y, 0, k_z)$ and $\theta_2(k_x, y, 0, k_z)$ using a double backstepping transformation. The transformation maps, for each k_x and k_z, the variables (Y, ω) into the variables (Ψ, Ω), that verify the following family of heat equations (parameterized in k_x, k_z).

$$\Psi_t = \epsilon\left(-\alpha^2 \Psi + \Psi_{yy}\right) - \beta\Psi - N\psi, \tag{100}$$

$$\Omega_t = \epsilon\left(-\alpha^2 \Omega + \Omega_{yy}\right) - \beta\Omega - N\Omega, \tag{101}$$

with boundary conditions

$$\Psi(t, k_x, 0, k_z) = \Psi(t, k_x, 1, k_z) = 0, \tag{102}$$

$$\Omega(t, k_x, 0, k_z) = \Omega(t, k_x, 1, k_z) = 0. \tag{103}$$

The transformation is defined as follows,

$$Y = \Psi - \int_0^y l(k_x, y, \eta, k_z)\Psi(t, k_x, \eta, k_z)\mathrm{d}\eta, \tag{104}$$

$$\begin{aligned} \omega &= \Omega - \int_0^y \theta_1(k_x, y, \eta, k_z)\Psi(t, k_x, \eta, k_z)\mathrm{d}\eta \\ &\quad - \int_0^y \theta_2(k_x, y, \eta, k_z)\Omega(t, k_x, \eta, k_z)\mathrm{d}\eta. \end{aligned} \tag{105}$$

Following Smyshlyaev and Krstic (2004, 2005), the functions $l(k_x, y, \eta, k_z)$, $\theta_1(k_x, y, \eta, k_z)$, and $\theta_2(k_x, y, \eta, k_z)$ are found as the solution of the following partial integro-differential equations,

$$\begin{aligned} \epsilon l_{\eta\eta} &= \epsilon l_{yy} - (\beta(k_x, y) - \beta(k_x, \eta))\, l - f \\ &\quad + \int_\eta^y f(k_x, y, \xi, k_z) l(k_x, \xi, \eta, k_z)\mathrm{d}\xi, \end{aligned} \tag{106}$$

$$\begin{aligned} \epsilon\theta_{1\eta\eta} &= \epsilon\theta_{1yy} - (\beta(k_x, y) - \beta(k_x, \eta))\,\theta_1 - h_1 \\ &\quad + h_1 \int_\eta^y l(k_x, \xi, \eta, k_z)\mathrm{d}\xi \\ &\quad + \int_\eta^y h_2(k_x, y, \xi, k_z)\theta_1(k_x, \xi, \eta, k_z)\mathrm{d}\xi, \end{aligned} \tag{107}$$

$$\begin{aligned} \epsilon\theta_{2\eta\eta} &= \epsilon\theta_{2yy} - (\beta(k_x, y) - \beta(k_x, \eta))\,\theta_2 - h_2 \\ &\quad + \int_\eta^y h_2(k_x, y, \xi, k_z)\theta_2(k_x, \xi, \eta, k_z)\mathrm{d}\xi. \end{aligned} \tag{108}$$

Eqs. (106)–(108) are hyperbolic partial integro-differential equation in the region $\mathcal{T} = \{(y, \eta) : 0 \le y \le 1, 0 \le \eta \le y\}$. Their boundary conditions are

$$l(k_x, y, y, k_z) = l(k_x, 1, \eta, k_z) = 0, \tag{109}$$

$$\theta_1(k_x, y, y, k_z) = \theta_1(k_x, 1, \eta, k_z) = 0, \tag{110}$$

$$\theta_2(k_x, y, y, k_z) = \theta_2(k_x, 1, \eta, k_z) = 0. \tag{111}$$

Remark 4. Eqs. (106)–(111) are well-posed and can be solved symbolically, by means of a successive approximation series, or numerically. See Smyshlyaev and Krstic (2004, 2005) for techniques in solving similar equations. Note that both (106) and (108) are autonomous. Hence, one must solve first for $l(k_x, y, \eta, k_z)$ and $\theta_2(k_x, y, \eta, k_z)$. Then the solution for l is plugged in (107) which then can be solved for $\theta_1(k_x, y, \eta, k_z)$. The observer gains are then found just by setting $\eta = 0$ in the kernels $l(k_x, y, \eta, k_z)$, $\theta_2(k_x, y, \eta, k_z)$ and $\theta_1(k_x, y, \eta, k_z)$.

Stability in the observed wave number range follows from stability of (100) and (101) and the invertibility of the transformation (104) and (105). The proof uses the same argument as in Smyshlyaev and Krstic (2004), slightly modified to account for a complex-valued kernel and using the fact that the terms are analytic in k. See Vazquez and Krstic (2007) for a detailed explanation.

5.2. Unobserved wave number analysis

When $k_x^2 + k_z^2 > M$, there is no output injection, as $\chi = 0$, and the linearized observer error verifies the following equations

$$\begin{aligned} \tilde{U}_t &= \frac{-\alpha^2 \tilde{U} + \tilde{U}_{yy}}{Re} - \beta\tilde{U} - U_y^e(y)\tilde{V} \\ &\quad - 2\pi k_x \mathrm{i}\tilde{P} + 2\pi k_z \mathrm{i} N\tilde{\phi} - N\tilde{U}, \end{aligned} \tag{112}$$

$$\tilde{V}_t = \frac{-\alpha^2 \tilde{V} + \tilde{V}_{yy}}{Re} - \beta\tilde{V} - \tilde{P}_y, \tag{113}$$

$$\begin{aligned} \tilde{W}_t &= \frac{-\alpha^2 \tilde{W} + W_{yy}}{Re} - \phi\tilde{W} - 2\pi k_z \mathrm{i}\tilde{P} \\ &\quad - 2\pi k_x \mathrm{i} N\tilde{\phi} - N\tilde{W}, \end{aligned} \tag{114}$$

the Poisson equation for the potential (51) and the continuity Eq. (50). Using the change of variables (88) and following the same steps as in Section 5.1, one gets the following equations for Y and ω.

$$Y_t = \epsilon\left(-\alpha^2 Y + Y_{yy}\right) - \beta Y - 2\pi k_x i U_y^e \tilde{V} + \alpha^2 \tilde{P} - NY, \tag{115}$$

$$\omega_t = \epsilon\left(-\alpha^2 \omega + \omega_{yy}\right) - \beta\omega - 2\pi k_z i U_y^e \tilde{V} - \alpha^2 N\tilde{\phi} - N\omega. \tag{116}$$

The Poisson equation for the potential is, in terms of ω,

$$-\alpha^2\tilde{\phi} + \phi_{yy} = \omega. \tag{117}$$

The boundary conditions for (115) and (116) are

$$Y(t, k_x, 0, k_z) = Y(t, k_x, 1, k_z) = 0, \tag{118}$$

$$\omega(t, k_x, 0, k_z) = \omega(t, k_x, 1, k_z) = 0, \tag{119}$$

$$\tilde{\phi}(t, k_x, 0, k_z) = \tilde{\phi}(t, k_x, 1, k_z) = 0. \tag{120}$$

Consider the Lyapunov function

$$\Lambda = \int_0^1 \frac{|\tilde{U}|^2 + |\tilde{V}|^2 + |\tilde{W}|^2}{2}\mathrm{d}y, \tag{121}$$

where we write, for short, $\int_0^1 f = \int_0^1 f(t, k_x, y, k_z)\mathrm{d}y$. The function Λ represents the L^2 norm (energy) of the observer error.

Denote by f^* the complex conjugate of f. Substituting Y and ω from (89) into (121), we get

$$\begin{aligned}\Lambda &= \int_0^1 4\pi^2\left[\frac{k_x^2|Y|^2 + k_z^2|W|^2 + k_xk_z(Y^*W + YW^*)}{2\alpha^4}\right.\\ &\quad\left.+\frac{k_z^2|Y|^2 + k_x^2|W|^2 - k_xk_z(Y^*W + YW^*)}{2\alpha^4}\right]\mathrm{d}y\\ &\quad+\int_0^1 \frac{|\tilde{V}|^2}{2}\mathrm{d}y\\ &= \int_0^1 \frac{|Y|^2 + |W|^2 + \alpha^2|\tilde{V}|^2}{2\alpha^2}\mathrm{d}y.\end{aligned} \tag{122}$$

Define then a new Lyapunov function,

$$\Lambda_1 = \alpha^2\Lambda = \int_0^1 \frac{|Y|^2 + |\omega|^2 + \alpha^2|\tilde{V}|^2}{2}\mathrm{d}y. \tag{123}$$

The time derivative of Λ_1 can be estimated as follows,

$$\begin{aligned}\dot{\Lambda}_1 &= -2\epsilon\alpha^2\Lambda_1 - \epsilon\int_0^1\left(|Y_y|^2 + |\omega_y|^2 + \alpha^2|\tilde{V}_y|^2\right)\\ &\quad- N\int_0^1\left(|Y|^2 + |\omega|^2\right) - \alpha^2 N\int_0^1\frac{\tilde{\phi}^*\omega + \tilde{\phi}\omega^*}{2}\\ &\quad+\int_0^1 \pi i U_y^e(y)\tilde{V}^*(2k_xY + k_z\omega)\\ &\quad-\int_0^1 \pi i U_y^e(y)\tilde{V}(2k_xY^* + k_z\omega^*)\\ &\quad+\alpha^2\int_0^1\frac{P^*Y + PY^* - P_y^*\tilde{V} - P_y\tilde{V}^*}{2}.\end{aligned} \tag{124}$$

For bounding (124), we use the following two lemmas.

Lemma 5.1. *For ω and $\tilde{\phi}$ verifying (116)–(120), the following holds.*

$$-\alpha^2\int_0^1\frac{\tilde{\phi}^*\omega + \tilde{\phi}\omega^*}{2} \le \int_0^1|\omega|^2. \tag{125}$$

Proof. The term we want to estimate is

$$-\alpha^2\int_0^1\frac{\tilde{\phi}^*\omega + \tilde{\phi}\omega^*}{2}. \tag{126}$$

Substituting $\alpha^2\phi$ from (117), (126) can be written as

$$-\int_0^1\frac{\tilde{\phi}_{yy}^*\omega + \tilde{\phi}_{yy}\omega^*}{2} + \int_0^1|\omega|^2. \tag{127}$$

Therefore, we need to prove that

$$\int_0^1\left(\tilde{\phi}_{yy}^*\omega + \tilde{\phi}_{yy}\omega^*\right) \ge 0. \tag{128}$$

Substituting ω from Eq. (117) into (128), we get

$$\begin{aligned}\int_0^1\left(\tilde{\phi}_{yy}^*\omega + \tilde{\phi}_{yy}\omega^*\right) &= \int_0^1|\tilde{\phi}_{yy}|^2 - \alpha^2\int_0^1\left(\tilde{\phi}_{yy}^*\tilde{\phi} + \tilde{\phi}_{yy}\tilde{\phi}^*\right)\\ &= \int_0^1|\tilde{\phi}_{yy}|^2 + \alpha^2\int_0^1|\tilde{\phi}_y|^2,\end{aligned} \tag{129}$$

which is nonnegative. □

Lemma 5.2. *Consider the function $U_y^e(y)$ as defined in (15). Then, the following holds:*

$$|U_y^e(y)| \le 4 + H. \tag{130}$$

Proof. Computing $U_y^e(y)$ from (15),

$$U_y^e(y) = H\frac{\cosh(Hy) - \cosh(H(1-y))}{2\sinh H/2 - \sinh H}. \tag{131}$$

Calling $g_1(y) = \cosh(Hy) - \cosh(H(1-y))$, since $g_1'(y) = H(\sinh(Hy) + \sinh(H(1-y)))$ is always positive for $y \in (0, 1)$, the maximum must be in the boundaries. Therefore,

$$|U_y^e(y)| \le g_2(H) = H\frac{\cosh H - 1}{\sinh H - 2\sinh H/2}. \tag{132}$$

One can rewrite g_2 as

$$g_2 = H\frac{\sinh H/2}{\cosh H/2 - 1}. \tag{133}$$

Since $g_2(0) = 4$, it suffices to verify that $g_2'(H) \le 1$.

$$g_2'(H) = \frac{g_3}{g_4} = \frac{\sinh H/2 - H^2/2}{\cosh H/2 - 1}. \tag{134}$$

This is equivalent to verify that $g_3 \le g_4$. Since $g_3(0) = g_4(0) = 0$, it is enough to prove $g_3' \le g_4'$, which comes from the fact that

$$g_3' = H/2\,(\cosh H/2 - 2H) \le H/2(\sinh H/2) = g_4', \tag{135}$$

because $\cosh x - 4x \le \sinh x$. □

Integrating by parts and applying Lemma 5.1,

$$\begin{aligned}\dot{\Lambda}_1 &\le -2\epsilon\alpha^2\Lambda_1 - \epsilon\int_0^1\left(|Y_y|^2 + |\omega_y|^2 + \alpha^2|\tilde{V}_y|^2\right)\\ &\quad+\int_0^1 \pi i U_y^e(y)\tilde{V}^*(k_xY + k_z\omega)\\ &\quad-\int_0^1 \pi i U_y^e(y)\tilde{V}(k_xY^* + k_z\omega^*) - N\int_0^1|Y|^2.\end{aligned} \tag{136}$$

Using Lemma 5.2 to bound U_y^e in (136),

$$\dot{\Lambda}_1 \leq -2\epsilon\left(1+\alpha^2\right)\Lambda_1 - N\int_0^1 |Y|^2 \mathrm{d}y + 2\pi\,(4+H)\int_0^1 \left(|\tilde{V}||k_x||Y| + |k_z||\omega|\right)\mathrm{d}y \leq \left(4+H-2\epsilon\left(1+\alpha^2\right)\right)\Lambda_1 \tag{137}$$

where we have applied Young's and Poincare's inequalities. Hence, if $\alpha^2 \geq \frac{4+H}{2\epsilon}$,

$$\dot{\Lambda}_1 \leq -2\epsilon\Lambda_1. \tag{138}$$

Dividing (138) by α^2 and using definition (123), we get that

$$\dot{\Lambda} \leq -2\epsilon\Lambda, \tag{139}$$

and stability in the unobserved wave number range follows when $k_x^2 + k_z^2 \geq M^2$ for M (conservatively) chosen as

$$M \geq \frac{1}{2\pi}\sqrt{\frac{(H+4)Re}{2}}. \tag{140}$$

5.3. Main result

The following result holds regarding the convergence of the observer.

Theorem 1. *Consider the system (21)–(23) and (6), with boundary conditions (7)–(10), and the system (24)–(33) with the gains* **L** *as computed in Section 5.1, and suppose that both have classical solutions. Then, the L^2 norms of $\tilde{U}, \tilde{V}, \tilde{W}$ converge to zero, i.e.,*

$$\lim_{t\to\infty}\int_{-\infty}^{\infty}\int_0^1\int_{-\infty}^{\infty}\left(\tilde{U}^2+\tilde{V}^2+\tilde{W}^2\right)(t)\mathrm{d}x\mathrm{d}y\mathrm{d}z = 0. \tag{141}$$

Proof. It is shown in Vazquez and Krstic (2007) (for a 2-D system possessing only one wave number) that if the origin of a (Fourier transformed) system is proven L^2 exponentially stable for every wave number, then the origin of the system is L^2 exponentially stable in physical space, i.e., considering all wave numbers together. A similar argument holds for our 3-D system with a set of two wave numbers.

We have established in Section 5.1 L^2 exponential stability for (56)–(58) in the observed wave range with the output injection gains computed using the backstepping method. In Section 5.2 we show that the unobserved wave range is also L^2 exponentially stable without output injection, by deriving a Lyapunov estimate (139). Hence all wave numbers are L^2 exponentially stable and physical stability follows as argued before. This means that we have

$$\int_{-\infty}^{\infty}\int_0^1\int_{-\infty}^{\infty}\left(\tilde{U}^2+\tilde{V}^2+\tilde{W}^2\right)(t)\mathrm{d}x\mathrm{d}y\mathrm{d}z \leq C_1\mathrm{e}^{-C_2 t}\int_{-\infty}^{\infty}\int_0^1\int_{-\infty}^{\infty}\left(\tilde{U}^2+\tilde{V}^2+\tilde{W}^2\right)(0)\mathrm{d}x\mathrm{d}y\mathrm{d}z, \tag{142}$$

for some $C_1 \geq 1$, $C_2 > 0$. Taking the limit as t goes to infinity in (142) gives us (141). □

Since we are dealing with a linearized version of the plant, this theorem has to be carefully interpreted. For a fully developed MHD flow (whether laminar or turbulent, if using the mean turbulent profile), with a Reynolds number possibly above the critical value (which for a MHD flow depends on N) but not too far above it, the observer is guaranteed to be convergent to the real velocity field, provided its initial estimates are not too far from the actual initial profile. Then convergence to the real pressure and electric potential follows.

Remark 5. See Sermange and Temam (1983) for a statement of well-posedness of MHD equations in bounded domains. However, there are no results about well-posedness of 3-D MHD equations in unbounded domains and such a study is beyond the scope of this paper. Hence we assume that the solutions for the velocity field, pressure and electric field, and their estimates, exist, are unique and regular enough for all statements and a priori estimates to make sense.

6. A nonlinear estimator

Since the original plant is nonlinear, we postulate a nonlinear observer to improve the convergence result of the linear estimator. This observer has the same structure and gains as the linear observer, but the nonlinear terms are added. In this we follow the design technique of the Extended Kalman Filter, in which gains are deduced for a linearized version of the plant and then used for a nonlinear observer.

The nonlinear observer equations are the following

$$\hat{U}_t = \frac{\triangle\hat{U}}{Re} - \hat{U}\hat{U}_x - \hat{V}\hat{U}_y - \hat{W}\hat{U}_z - \hat{P}_x + N\hat{\phi}_z - N\hat{U} - Q^U, \tag{143}$$

$$\hat{V}_t = \frac{\triangle\hat{V}}{Re} - \hat{U}\hat{V}_x - \hat{V}\hat{V}_y - \hat{W}\hat{V}_z - \hat{P}_y - Q^V, \tag{144}$$

$$\hat{W}_t = \frac{\triangle\hat{W}}{Re} - \hat{U}\hat{W}_x - \hat{V}\hat{W}_y - \hat{W}\hat{W}_z - \hat{P}_z - N\hat{\phi}_x - N\hat{W} - Q^W. \tag{145}$$

The estimated potential is computed from

$$\triangle\hat{\phi} = \hat{U}_z - \hat{W}_x, \tag{146}$$

and the observer verifies the continuity equation,

$$\hat{U}_x + \hat{V}_y + \hat{W}_z = 0, \tag{147}$$

and Dirichlet boundary conditions,

$$\hat{U}(t,x,0,z) = \hat{W}(t,x,0,z) = \hat{V}(t,x,0,z) = 0, \tag{148}$$

$$\hat{U}(t,x,1,z) = \hat{W}(t,x,1,z) = \hat{V}(t,x,1,z) = 0, \tag{149}$$

$$\hat{\phi}(t,x,0,z) = \hat{\phi}(t,x,1,z) = 0. \tag{150}$$

The estimated current field is computed from the other estimated variables using a copy of Eqs. (11)–(13).

$$\hat{j}^x(t,x,y,z) = -\hat{\phi}_x - \hat{W}, \tag{151}$$

$$\hat{j}^y(t,x,y,z) = -\hat{\phi}_y, \tag{152}$$

$$\hat{j}^z(t,x,y,z) = -\hat{\phi}_z + \hat{U}. \tag{153}$$

In Eqs. (143)–(145), the Q terms are the same as for the linear observer. Hence, the observer is designed for the linearized plant and then the linear gains are used for the nonlinear observer. Such a nonlinear observer will produce closer estimates of the states in a larger range of initial conditions.

Using the fluctuation variable and the observer error variables, we can write the nonlinear observer velocity field error equations as follows.

$$\tilde{U}_t = \frac{\triangle\tilde{U}}{Re} - U^e(y)\tilde{U}_x + \mathcal{N}^U(\tilde{U},\tilde{V},\tilde{W},u,V,W) - U_y^e(y)\tilde{V} - \tilde{P}_x + N\tilde{\phi}_z - N\tilde{U} + Q^U, \tag{154}$$

$$\tilde{V}_t = \frac{\triangle\tilde{V}}{Re} - U^e(y)\tilde{V}_x + \mathcal{N}^V(\tilde{U},\tilde{V},\tilde{W},u,V,W) - \tilde{P}_y + Q^V, \tag{155}$$

$$\tilde{W}_t = \frac{\triangle\tilde{W}}{Re} - U^e(y)\tilde{W}_x + \mathcal{N}^W(\tilde{U},\tilde{V},\tilde{W},u,V,W) - \tilde{P}_z - N\tilde{\phi}_x - N\tilde{W} + Q^W, \tag{156}$$

where we have introduced

$$\mathcal{N}^U = \tilde{U}\tilde{U}_x - u\tilde{U}_x - \tilde{U}u_x + \tilde{V}\tilde{U}_y - V\tilde{U}_y - \tilde{V}u_y + \tilde{W}\tilde{U}_z - W\tilde{U}_z - \tilde{W}u_z, \quad (157)$$

$$\mathcal{N}^V = \tilde{U}\tilde{V}_x - u\tilde{V}_x - \tilde{U}V_x + \tilde{V}\tilde{V}_y - V\tilde{V}_y - \tilde{V}V_y + \tilde{W}\tilde{V}_z - W\tilde{V}_z - \tilde{W}V_z, \quad (158)$$

$$\mathcal{N}^W = \tilde{U}\tilde{W}_x - u\tilde{W}_x - \tilde{U}W_x + \tilde{V}\tilde{W}_y - V\tilde{W}_y - \tilde{V}W_y + \tilde{W}\tilde{W}_z - W\tilde{W}_z - \tilde{W}W_z. \quad (159)$$

Assuming, for the purposes of observer design and analysis, that the observer state $(\hat{U}, \hat{V}, \hat{W})$ is close to the actual state (U, V, W) (i.e., the error state is close to zero), and that the fluctuation (u, V, W) around the equilibrium state is small, then $\mathcal{N}_U(\tilde{U}, \tilde{V}, \tilde{W}, u, V, W)$, $\mathcal{N}_V(\tilde{U}, \tilde{V}, \tilde{W}, u, V, W)$ and $\mathcal{N}_W(\tilde{U}, \tilde{V}, \tilde{W}, u, V, W)$ are small and dominated by the linear terms in the equations, so they can be neglected. The linearized error equations are then

$$\tilde{U}_t = \frac{\triangle\tilde{U}}{Re} - U^e(y)\tilde{U}_x - U^e_y(y)\tilde{V} - \tilde{P}_x + N\tilde{\phi}_z - N\tilde{U} + Q^U, \quad (160)$$

$$\tilde{V}_t = \frac{\triangle\tilde{V}}{Re} - U^e(y)\tilde{V}_x - \tilde{P}_y + Q^V, \quad (161)$$

$$\tilde{W}_t = \frac{\triangle\tilde{W}}{Re} - U^e(y)\tilde{W}_x - \tilde{P}_z - N\tilde{\phi}_x - N\tilde{W} + Q^W, \quad (162)$$

which are the same as (37)–(39). Thus, as expected, the error equations for the observer designed for the linearized plant, and the linearized error equations for the nonlinear observer are the same; this is the main reason why the same gains derived in Section 5 are used.

Remark 6. Note that we have not defined $\tilde{u}$ for the nonlinear observer, since $\tilde{u} = \tilde{U} - \tilde{U}^e = (U - \hat{U}) - (U^e - \hat{U}^e) = U - \hat{U} = \tilde{U}$, i.e., $\tilde{U}^e = 0$, because by definition $U^e = \hat{U}^e$. This implies that *any* function $U^e(y)$ can be used in the design of the nonlinear observer, even if it is not a true equilibrium, without any changes in the observer structure. This is not the case for the observer designed in Sections 4 and 5 for the linearized system, where a nonequilibrium $U^e(y)$ would produce forcing (nonhomogeneous) terms in both the linearized system and the observer. Following Chevalier et al. (2006), we may consider the *mean turbulent profile* instead of considering the exact *laminar* equilibrium profile. This amounts to changing U^e in definition (15). Since U^e appears in Eqs. (90)–(93), which are used to compute output injection gains in Eqs. (106)–(108), the observer gains will change (quantitatively) for the turbulent mean profile.

7. Concluding remarks

We have presented an observer that estimates velocity, pressure, electric potential and current in a Hartmann flow, characterized by an electrically conducting fluid moving between parallel plates in the presence of an imposed transverse magnetic field. The estimator consists of a copy of the linearized MHD equations, combined with linear injection of output estimation error, with observer gains designed using backstepping in Fourier space. Pressure, skin friction and current measurements from the lower wall are used for output injection.

The convergence result stated in Theorem 1 guarantees asymptotic convergence of the estimated states to the actual values of the *linearized* plant. For this to be true for the *nonlinear* plant, the estimates have to be initialized close enough to the real initial values and the MHD system has to stay in a neighborhood of the equilibrium at all times. We have presented a nonlinear observer in Section 6 that incorporates the nonlinearities of the plant. It is expected that the nonlinear observer will allow larger discrepancies between the state and the profile while still producing valid estimates. The nonlinear observer also allows to use, as in Chevalier et al. (2006), the mean turbulent profile instead of the exact laminar equilibrium profile, only needing a quantitative change of the observer gains. For the estimates obtained using the mean turbulent profile to be good enough we would need similar assumptions as those given in Theorem 1, meaning now that the state has to stay close enough to the mean turbulent profile at all times.

In case that $N = 0$, meaning that either there is no imposed magnetic field or the fluid is nonconducting, Eqs. (2)–(4) are the Navier–Stokes equations and the observer reduces to a velocity/pressure estimator for a 3-D channel flow. This is a result of high interest on its own that can be seen as dual to the channel flow control problem, which was solved in Cochran et al. (2006) using similar tools. Some physical insight can be gained analyzing this case. In the context of hydrodynamic stability theory, the linearized observer error system written in (Y, ω) variables verify equations analogous to the classical Orr–Sommerfeld–Squire equations. These are Eqs. (98) and (99) for observed wave numbers and Eqs. (115) and (116) for unobserved wave numbers. As in Cochran et al. (2006), we use the backstepping transformations (104) and (105) not only to stabilize (using gain l) but also to decouple the system (using gains θ_1, θ_2) in the small wave number range, where nonnormality effects are more severe. Even if the linearized system is stable, nonnormality produces large transient growths (Reddy, Schmid, & Henningson, 1993; Schmid & Henningson, 2001), which enhanced by nonlinear effects may allow the error system to go far away from the origin, producing inaccurate estimates. This warrants the use of extra gains to map the system into two uncoupled heat equations (100) and (101).

References

Aamo, O. M., & Krstic, M. (2002). *Flow control by feedback: Stabilization and mixing*. Berlin: Springer.

Baker, J., Armaou, A., & Christofides, P. D. (2000). Nonlinear control of incompressible fluid flow: Application to Burgers' equation and 2D channel flow. *Journal of Mathematical Analysis and Applications*, *252*, 230–255.

Baker, J., & Christofides, P. (2002). Drag reduction in transitional linearized channel flow using distributed control. *International Journal of Control*, *75*, 1213–1218.

Balogh, A., Liu, W.-J., & Krstic, M. (2001). Stability enhancement by boundary control in 2D channel flow. *IEEE Transactions on Automatic Control*, *46*, 1696–1711.

Bamieh, B., Paganini, F., & Dahleh, M. A. (2000). Distributed control of spatially-invariant systems. *IEEE Transactions on Automatic Control*, *45*, 1091–1107.

Barbu, V. (2006). Stabilization of a plane channel flow by wall normal controllers. Preprint.

Barbu, V., Popa, C., Havarneanu, T., & Sritharan, S. S. (2003). Exact controllability of magneto-hydrodynamic equations. *Communications on Pure and Applied Mathematics*, *56*(6), 732–783.

Berger, T. W., Kim, J., Lee, C., & Lim, J. (2000). Turbulent boundary layer control utilizing the Lorentz force. *Physics of Fluids*, *12*, 631.

Breuer, K. S., & Park, J. (2004). Actuation and control of a turbulent channel flow using Lorentz forces. *Physics of Fluids*, *16*(4), 897.

Chevalier, M., Hoepffner, J., Bewley, T. R., & Henningson, D. S. (2006). State estimation in wall-bounded flow systems. Part 2. Turbulent flows. *Journal of Fluid Mechanics*, *552*, 167–187.

Cochran, J., Vazquez, R., & Krstic, M. (2006). Backstepping boundary control of Navier–Stokes channel flow: A 3D extension. In *Proceedings of the 25th American control conference* (pp. 876–881).

Debbagh, K., Cathalifaud, P., & Airiau, C. (2007). Optimal and robust control of small disturbances in a channel flow with a normal magnetic field. *Physics of Fluids*, *9*(1), 014103–014103.

Hoepffner, J., Chevalier, M., Bewley, T. R., & Henningson, D. S. (2005). State estimation in wall-bounded flow systems. Part 1. Perturbed laminar flows. *Journal of Fluid Mechanics*, *534*, 263–294.

Hogberg, M., Bewley, T. R., & Henningson, D. S. (2003). Linear feedback control and estimation of transition in plane channel flow. *Journal of Fluid Mechanics*, *481*, 149–175.
Jovanovic, M. R., & Bamieh, B. (2005). Componentwise energy amplification in channel flows. *Journal of Fluid Mechanics*, *543*, 145–183.
Krstic, M., Kanellakopoulos, I., & Kokotovic, P. V. (1995). *Nonlinear and adaptive control design*. New York: Wiley.
Lee, D., & Choi, H. (2001). Magnetohydrodynamic turbulent flow in a channel at low magnetic Reynolds number. *Journal of Fluid Mechanics*, *439*, 367–394.
Muller, U., & Buhler, L. (2001). *Magnetofluiddynamics in channels and containers*. Berlin: Springer.
Pang, J., & Choi, K.-S. (2004). Turbulent drag reduction by Lorentz force oscillation. *Physics of Fluids*, *16*(5), L35.
Reddy, S. C., Schmid, P. J., & Henningson, D. S. (1993). Pseudospectra of the Orr–Sommerfeld operator. *SIAM Journal on Applied Mathematics*, *53*(1), 15–47.
Schmid, P. J., & Henningson, D. S. (2001). *Stability and transition in shear flows*. Berlin: Springer.
Schuster, E., & Krstic, M. (2003). Inverse optimal boundary control for mixing in magnetohydrodynamic channel flows. In *Proceedings of the 2003 CDC* (pp. 3966–3971).
Sermange, M., & Temam, R. (1983). Some mathematical questions related to the MHD equations. *Communications on Pure and Applied Mathematics*, *36*, 635–664.
Smyshlyaev, A., & Krstic, M. (2004). Closed form boundary state feedbacks for a class of partial integro-differential equations. *IEEE Transactions on Automatic Control*, *49*, 2185–2202.
Smyshlyaev, A., & Krstic, M. (2005). Backstepping observers for parabolic PDEs. *Systems and Control Letters*, *54*, 1953–1971.
Sritharan, S. S., Barbu, V., Havarneanu, T., & Popa, C. (2005). Local controllability for the magnetohydrodynamic equations revisited. *Advances in Differential Equations*, *10*(5), 481–504.
Thibault, J.-P., & Rossi, L. (2003). Electromagnetic flow control: Characteristic numbers and flow regimes of a wall-normal actuator. *Journal of Physics D (Applied Physics)*, *36*, 2559–2568.
Triggiani, R. (2007). Stability enhancement of a 2-D linear Navier–Stokes channel flow by a 2-D, wall-normal boundary controller. *Discrete and Continuous Dynamical Systems—Series B*, *8*(2), 279–314.
Vazquez, R., & Krstic, M. (2007). A closed-form feedback controller for stabilization of the linearized 2-D Navier–Stokes Poiseuille system. *IEEE Transactions on Automatic Control*, *52*, 2298–2312.
Vazquez, R., & Krstic, M. (2005). A closed-form observer for the channel flow Navier–Stokes system. In *Proceedings of the 2005 CDC* (pp. 5959–5964).

Rafael Vazquez received the Ph.D. and M.S. degrees in aerospace engineering from the University of California, San Diego, and B.S. degrees in electrical engineering and mathematics from the University of Seville, Spain.

He is assistant professor in the Aerospace and Fluid Mechanics Department in the University of Seville, Spain. Vazquez is a coauthor of the book Control of Turbulent and Magnetohydrodynamic Channel Flows (2007). He was a CTS Marie Curie Fellow at the Université Paris-Sud (2005). His research interests include nonlinear control, control of distributed parameter systems, dynamical systems, and applications to flow control, orbital mechanics, air traffic control and nanomechatronics. He has been finalist for the Best Student Paper Award in the 2005 CDC.

Eugenio Schuster is Assistant Professor of Mechanical Engineering and Mechanics at Lehigh University. He holds undergraduate degrees in Electronic Engineering (Buenos Aires University, Argentina, 1993) and Nuclear Engineering (Balseiro Institute, Argentina, 1998). He obtained his M.S. (2000) and Ph.D. (2004) degrees at University of California San Diego. Schuster is the recipient of the NSF Career Award. His research interests are in distributed parameter and nonlinear control systems, with applications that include fusion reactors, plasmas, and magnetohydrodynamic flows.

Miroslav Krstic is the Sorenson Professor of Mechanical and Aerospace Engineering and the Director of the newly formed Center for Control, Systems, and Dynamics (CCSD) at UCSD. Krstic is a coauthor of the books Nonlinear and Adaptive Control Design (1995), Stabilization of Nonlinear Uncertain Systems (1998), Flow Control by Feedback (2002), Real Time Optimization by Extremum Seeking Control (2003), and Control of Turbulent and Magnetohydrodynamic Channel Flows (2007). He received the NSF Career, ONR YI, and PECASE Awards, as well as the Axelby and the Schuck paper prizes. In 2005 he was the first engineering professor to receive the UCSD Award for Research. Krstic is a Fellow of IEEE, a Distinguished Lecturer of the Control Systems Society, and a former CSS VP for Technical Activities. He has served as AE for several journals and is currently Editor for Adaptive and Distributed Parameter Systems in Automatica.